



HAL
open science

Bioengineered Human Organ-on-Chip Reveals Intestinal Microenvironment and Mechanical Forces Impacting Shigella Infection

Alexandre Grassart, Valérie Malardé, Samy Gobaa, Anna Sartori-Rupp, Jordan Kerns, Katia Karalis, Benoit Marteyn, Philippe Sansonetti, Nathalie Sauvonnet

► To cite this version:

Alexandre Grassart, Valérie Malardé, Samy Gobaa, Anna Sartori-Rupp, Jordan Kerns, et al.. Bioengineered Human Organ-on-Chip Reveals Intestinal Microenvironment and Mechanical Forces Impacting Shigella Infection. *Cell Host and Microbe*, 2019, 26 (3), pp.435-444.e4. 10.1016/j.chom.2019.09.007 . pasteur-02579884

HAL Id: pasteur-02579884

<https://pasteur.hal.science/pasteur-02579884>

Submitted on 3 Jun 2020

HAL is a multi-disciplinary open access archive for the deposit and dissemination of scientific research documents, whether they are published or not. The documents may come from teaching and research institutions in France or abroad, or from public or private research centers.

L'archive ouverte pluridisciplinaire **HAL**, est destinée au dépôt et à la diffusion de documents scientifiques de niveau recherche, publiés ou non, émanant des établissements d'enseignement et de recherche français ou étrangers, des laboratoires publics ou privés.

A bioengineered human Organ-on-Chip reveals that mechanical forces and 3D microenvironment of the intestinal epithelium are critical for *Shigella* infection.

Alexandre Grassart^{1*}, Valérie Malardé¹, Samy Gobba^{2*}, Anna Sartori-Rupp^{3*}, Jordan Kerns⁴, Katia Karalis⁴, Benoit Marteyn^{1,5}, Philippe Sansonetti¹ and Nathalie Sauvonnet^{1*}.

¹ Unité de Pathogénie Microbienne Moléculaire, Institut Pasteur, INSERM U1202.

28, rue du Docteur Roux, 75015, Paris, France

² Biomaterials and Microfluidics Facility, C2RT, Institut Pasteur, 28 rue du Docteur Roux, 75015, Paris, France

³ Unité de Bio-imagerie ultra-structurale, C2RT, Institut Pasteur, 28, rue du Docteur Roux, 75015, Paris, France

⁴ Emulate, Inc., 27 Drydock Avenue, Boston, MA 02210 USA

⁵ IBMC, Université de Strasbourg, CNRS UPR 9002 (ARN)

* These authors contributed equally to this work

*Corresponding authors:

alexandre.grassart@pasteur.fr

nathalie.sauvonnet@pasteur.fr

Key words

Organ-on-chip, Intestine-Chip, host-pathogen interactions, intestine, microengineering, peristalsis, enterocyte, shear stress, stretching.

Highlights

- An Organ-on-Chip approach for studying host pathogen interactions
- *Shigella* infects enterocytes extremely efficiently from the intestinal lumen

- The crypt-like structure of the intestine is critical for *Shigella* adhesion
- Peristaltic motion (mechanical forces) enhances *Shigella* invasion
- Recreating the 3D microenvironment and physiological forces of the intestine enables the high level of *Shigella* virulence found in human individuals to be recreated in the Organ-Chip

Summary

Intestinal epithelial cells are constantly exposed to pathogens and mechanical forces. However, the impact of mechanical forces on infections leading to diarrheal diseases remains largely unknown. Here, we addressed whether flow and peristalsis impact the infectivity of the human pathogen *Shigella* within a 3D colonic epithelium using Intestine-Chip technology. Strikingly, the infection was significantly increased and minimal bacterial loads were sufficient to invade enterocytes from the apical side and to trigger loss of barrier integrity, thereby shifting the paradigm about the early stage of *Shigella* invasion. We found that *Shigella* quickly colonize epithelial crypt-like invaginations and demonstrates the essential role of the microenvironment. Furthermore, by modulating the mechanical forces, we uncovered the impact of peristalsis on *Shigella* invasion. Collectively, our results reveal that *Shigella* takes advantage of the micro-architecture and mechanical forces, i.e. leverages the intestinal microenvironment in order to invade the intestine. This approach opens new avenues for studying infection of human restricted enteric pathogens.

Introduction

The human intestine is lined by a monolayer of epithelium, which acts as a gatekeeper against infectious microorganisms. During the past decades, much has been learned regarding the molecular machineries leveraged or employed by pathogens to invade this epithelial barrier (Ferrari and Sansonetti, 2016). Though, how pathogens interact with their host at the tissue microenvironment remains elusive. Although growing evidence indicates that physical forces can alter the pathogenicity of bacteria, as illustrated by the pioneering work revealing that the shear stress encountered in the urinary tract enhanced type 1 fimbriae-mediated *Escherichia coli* bacterial adhesion (Thomas et al., 2002), the role of the mechanical forces on host-pathogen interactions remains hard to assess.

Shigella flexneri is an enteroinvasive bacterium inducing bacillary dysentery restricted to the human colon. At the molecular and cellular levels, *Shigella* invasion depends on a type III secretion system (T3SS) that translocates about 30 effector proteins into the cytosol of its target cell (Parsot, 2009). Inside its host cell, the bacteria lyses its vacuolar membrane, replicates, spreads into adjacent cells and reprograms cells to express pro-inflammatory mediators (Ashida et al., 2015), resulting in the destruction of the epithelium. Moreover *Shigella* does not express flagellum or adhesin albeit IcsA was shown in some conditions to confer to the bacterium adhesive functions (Brotcke Zumsteg et al., 2014). Although lack of these apparatuses could be advantageous to escape the immune response, it might also be a drawback with respect to adherence and invasion capacities. As well known, the intestinal epithelium continuously imposes two main physical forces on a colonizing pathogen, i.e. shear stress induced by the intestinal flow, and tensile forces induced by stretching of the underlying muscle layer and resulting in the peristalsis, that may overcome the infectivity of pathogens (Gayer and Basson, 2009; Womack et al., 1987).

While the intracellular life of *Shigella* has been extensively studied in single cell models, few studies have provided a mechanistic view of the pathogen-colonic tissue interactions (Arena et al., 2015), primarily due to the difficulty of real-time imaging of transient events *in vivo*, using human relevant small-animal models. Moreover, clinical data clearly show that the ingestion of only few hundreds of bacteria is sufficient to trigger diarrheal symptoms in humans (DuPont et al., 1989; Kotloff et al., 1995). However, *Shigella* is notoriously inefficient in infecting polarized epithelial monolayers from the apical surface in the standard, static *in vitro* models (i.e. TranswellTM system) using either human colon cell line (Mounier et al., 1992) or the recently developed enteroids from human colorectal biopsies (Koestler et al., 2019; Ranganathan et al., 2019). This gap between *in vivo* and *in vitro* results might reflect the oversimplification of the intestinal epithelial microenvironment in the conventional *in vitro* models. Recently, advances in Organ-on-Chip technology and microengineering have demonstrated the increased capabilities to recreate important aspects of the intestinal barrier physiology *in vitro* (Kim and Ingber, 2013; Kim et al., 2016). In this study, we employ this approach and use the Intestine-Chip to study *S. flexneri* infection and demonstrate that *in vivo*-like mechanical forces increase the capability of this bacterium to invade the human colonic epithelium.

Results

We set up an Organ-on-Chip approach that recreates a human 3D colonic epithelium and its micro-environmental physical cues (luminal fluidic flow and peristaltic motions) as previously published (Kim et al., 2016). Briefly, we used the Intestine-Chip system made of an elastomeric polymer polydimethylsiloxane (PDMS) (Figure 1A) which consists of: (i) a central channel separated vertically by a stretchable porous membrane, (ii) two hollow vacuum channels framing laterally the central channel (Figure 1B). The application of cyclic vacuum within these channels induces strain and stretching of the porous membrane that

recreate peristaltic-like motions (Kim et al., 2016; Kim and Ingber, 2013). To support the culture of human colonic epithelial cells (Caco-2 cell line, clone TC7), the separating membrane was coated with extra cellular matrix (ECM). To recapitulate the physiological microenvironment of the intestine the seeded cells were exposed for 5 to 6 days to continuous flow (30uL/hour, about $0.0009 \text{ dyne cm}^{-2}$) to recreate the sheer stress on the apical side of the epithelium and to cyclic mechanical strain (10% at a frequency of 0.15Hz) to reproduce the peristaltic motions (Chaturvedi et al., 2008; Gayer and Basson, 2009; Kim et al., 2012; Womack et al., 1987). Cells grown under these conditions self-organized into villi-like structures interspaced by crypt-like invaginations (Figures 1C and S1A) as previously shown (Kim and Ingber, 2013). In a first step, we confirmed that the seeded Caco-2 cells were polarized and exhibited known differentiation markers (E-cadherin, villin, FABP1- KRT20) (Figures 1C, S1B, S1C). Scanning electron microscopy (SEM) imaging also showed microvilli on the apical surface, a typical structural marker of differentiated and polarized enterocytes (Figure 1G). The multicellular villi/crypt-like tissue architecture was also clearly visible by SEM. Finally, we confirmed the impermeability of the epithelial barrier by measuring the diffusion of Dextran-FITC through the monolayer (Figure S1D). Therefore, Intestine-Chip cultures developed a differentiated and mature, 3D enterocyte cytoarchitecture. In order to address whether *Shigella flexneri* could infect the human colon epithelium in the chip, we introduced a wild-type strain expressing GFP (*Shigella*-WT-GFP) in the intestinal lumen of an Intestine-Chip; images were acquired at 30, 60 and 120 minutes post inoculation (Figures 1D, 1E, S2A) While individual *S. flexneri* were hardly visible at 30 min using epifluorescence microscopy, we observed a preferential enrichment of *Shigella*-WT-GFP within the interstitial spaces between villi-like structures at one and two hours following inoculation (Figures 1D, 1E, S2A). By analyzing fluorescent microscopy images for the distribution of *Shigella* associated with the epithelium surface at one-hour post challenge, we

found that about 80% of bacteria were located within interstitial spaces (Figures 1E-F). We also confirmed these results at an ultrastructural level in which a majority of *Shigella* (about 70%) was also localized within crypt-like structures (Figure 1H-I). To test whether this specific localization or homing is reflecting operation of an active mechanism or not, we interrogated the distribution of fluorescent polystyrene beads at the epithelial surface. We observed that a majority of beads were similarly abundant within interstitial spaces, albeit to a lesser extent than the bacteria (Fig. 1D, I). Taken together, these results suggest that *Shigella* is most likely passively trapped within these intestinal tissue-specific spaces. This precise localization is reminiscent of *in vivo* observations indicating the association of *S. flexneri* with the crypts of colonocytes early in the infection process (Arena et al., 2015). However, we found that these sites were permissive for bacterial colonization, only under physiological luminal flow rates, since a 10-fold increase in flow abrogated the bacterial enrichment (Figures S1E-F). Finally, we tested whether *Shigella* could actually invade the epithelium. To do so, we introduced *Shigella*-WT-GFP in the chip lumen using a multiplicity of infection (MOI) of 1 at 37°C under physiological flow and peristaltic motion. Two hours later, non-adhering bacteria were washed away and the infection was left to continue overnight. We observed a strong propagation of *Shigella*-WT-GFP within the entire central channel of the chip (Figures 1J-L). Furthermore, bacterial invasion was associated with significant changes in epithelium morphology, including loss of the villi-like 3D structures. Specifically, cross sections imaging of the infected chip showed a striking destruction of the epithelial monolayer (Figure 1K) and a significant decrease of approximately 75 % in the villi-like height (Figure 1M). We also were able to clearly detect *Shigella* inside the remaining cells, as confirmed by intra/extracellular bacterial immunostaining (Figure S2B), as well as in the pores of the PDMS membrane that supports the epithelial cell culture (Figure 1K). These results clearly indicate a directional and polarized infection from the apical to the bottom of

the epithelial invaginations, in agreement with *in vivo* data showing spreading of *Shigella* across the whole colonic mucosal depth over time. However, it should be noted that disrupting cellular junctions by chelating calcium (EGTA), thereby allowing access to the basolateral side of the monolayer, increased the invasion of *S. flexneri* by 18 fold (Figure S4D). Importantly, we also observed that the non-invasive *Shigella-mxiD*-GFP mutant strain that does not secrete *Shigella* effectors, although recruited in the epithelial invaginations, neither led to foci formation nor to destruction of the epithelium morphology, as compared to the *Shigella*-WT-GFP (Figures 1J, 1L). Thus, the invasion of the Intestine-Chip with *Shigella* WT-GFP is T3SS-dependent. Moreover, infection with an *icsA* mutant strain of *Shigella*, a motility deficient mutant (Bernardini et al., 1989) that is lacking cell-to-cell spreading capacity, although it led to cell infection it did not result in the formation of large foci of epithelial destruction (Figure S3C). Altogether, these results show that the Intestine-Chip microenvironment recapitulates the main characteristics of *S. flexneri* invasion of the enterocyte monolayer *in vivo*.

To assess the importance of the colon 3D environment, we performed *S. flexneri* infection on Caco-2 cells cultured *in vitro* on conventional TranswellTM for 3 weeks, using a MOI of 1 or 100. As previously observed, wild type *S. flexneri* failed to efficiently infect the polarized Caco-2 cells-based monolayer on TranswellTM, introduced from the apical side of the culture (Figure 2B)(Mounier et al., 1992). To quantify the efficiency of *S. flexneri* invasion, we introduced WT bacteria apically to monolayers either matured on Transwell or on Intestine-Chip and after 2h of invasion, extracellular bacteria were eliminated by gentamycin treatment for 1 h before plating and counting the colonies (CFU, Figure 2B). Strikingly, maturation in the Intestine-Chip enhanced the *Shigella* invasion by 10,000 fold, as compared to the Transwell (Figure 2B). We also infected flat epithelium grown for only 2 days in the Intestine-Chip under flow and peristalsis, a maturation stage where no 3D villi-like

formations are visible yet, we did not observe any infection foci (Figure 2A). Altogether, these results reveal that a 3D-like architecture is essential for efficient *S. flexneri* invasion of the epithelium at the early stages of infection.

In a second step, we wanted to further explore the sensitivity of the Intestine-Chip system for *Shigella* infection. Thus, we exposed the epithelium to various inoculation densities, using a range from 100,000 down to only 100 *Shigella*-WT-GFP bacteria (corresponding to MOI of 1 to MOI of 0.001 respectively), for 2 hours and assessed its invasion using a protective assay strategy. After washing and overnight incubation with gentamicin, we observed that wild-type *Shigella* was highly efficient in invading the colonic epithelium (Figures 2C-D). Strikingly, even a few hundreds of bacteria were sufficient to generate infection foci (Figures 2C-D) in the Intestine-Chip, an efficiency close to the data reported from the clinic (DuPont et al., 1989). This suggests that the Intestine-Chip can recapitulate essential cues of the human colonic microenvironment required for *Shigella* infection.

Next, we performed live imaging in order to gain insights into the infection dynamics. We analyzed the expansion of bacterial foci into the epithelial barrier, leading to the consecutive invasion of bacteria into the lower channel (Figures 2E-F). With this experiment we demonstrated that foci could indeed be initiated from a single bacterium alone and revealed that epithelial barrier can be crossed by *Shigella* around 5 hours post-initiation of the infection. By measuring the number of bacteria over time, we estimated that the epithelium was disrupted when these foci reached a density of approximately 70 bacteria (Figure 2F). Importantly, the bacterial appearance into the basal channel was not linked to a major leakage since 70kDa Dextran-FITC was not recovered in the basal channel of infected chips. (Figure S1D). Furthermore, we observed that polystyrene beads (1µm in diameter) also failed to cross through the pores of the supporting membrane during infection (Figure S4A). Finally, we observed that the crossing of *S. flexneri* through the epithelial barrier did not result from

massive cells apoptosis (Figure S4B). These data indicate that *Shigella* propagation and crossing through the monolayer is a direct intracellular mechanism and not a paracellular and passive one.

Then, we addressed whether recapitulation of the physiological mechanical forces (shear stress and peristaltic motions) in the 3D- and 2D-matured intestinal epithelial layer, had an impact on the *Shigella* infection process. To better understand their roles in virulence, we interrogated each of these parameters at different key steps of the infection: bacterial adhesion, invasion and propagation (Figures 3, 4). First, we analyzed the adhesion step by apically exposing Intestine-Chips to *Shigella* for one hour to avoid most of their uptake (Figures 3A-C). We did not observe any significant difference in CFU between the different conditions tested (Figure 3B). However, bacteria at this stage of infection remain extracellular and gentamycin protection could not be performed to distinguish bacteria that failed to be washed away. Thus, CFU values might reflect the presence of a mixture of adherent and non-adherent bacteria. To circumvent this technical limitation, we also analyzed images from Intestine-Chip sections, we could wash more extensively. In addition, we also took advantage of a modified *S. flexneri* strain encoding a transcription-based secretion activity reporter (TSAR) that expresses GFP only upon T3SS induction, that should occur when *Shigella* gets in contact with the host cell (Campbell-Valois et al., 2014). By counting the number of bacteria that were T3SS activated (GFP positive), we observed a drastic difference between 3D and 2D monolayers, regardless of other physical stimuli (Figure 3A, 3C). This result demonstrates that *S. flexneri* adhesion to the cell is dependent on the tissue microenvironment, in particular on the crypt-like structures. In addition, the putative *S. flexneri* adhesin, IcsA, had no impact on the number of adhering bacteria (Figure S3B). Then, we analyzed the role of the microenvironment and mechanical forces in the invasion step : the uptake of *Shigella* into epithelial cells. To do so, we challenged apically Intestine-Chips with bacteria for 2h,

washed and eliminated remaining extracellular bacteria by gentamycin treatment for another hour before plating and counting CFUs (Figure 3D-E). Strikingly, we observed a strong invasion only in 3D epithelium that was mechanically stimulated by stretching tensile forces (Fig. 3D, E). This indicates that apical invasion of the epithelium by *Shigella* strongly depends on peristaltic motions. Finally, we analyzed the impact of each of these conditions in the capacity of *S. flexneri* propagation in Intestine-Chips protected by gentamycin for 13 hours after an initial infection challenge for 2 hours (Figure 4). As expected, we observed an important increase of CFUs (around 10^6 CFUs, about 15-fold increase) as compared to the invasion time point, although only in infected 3D cultured Intestine-Chips. However, we noticed that the absence of any mechanical stimulation (such as flow and stretch) limited the bacterial propagation by 60 % (Figures 4A-B). This suggests that mechanical forces exerted by both flow and stretching enhance the bacterial propagation in the 3D monolayers. To better fine tune the propagation step, we analyzed the area of the bacterial invasion, by performing an image analysis of 3D-matured Intestine-Chips infected as previously, although at a low bacterial inoculum (MOI 0.05) in order to be able to precisely quantify the number of bacterial foci (Figures 4C-E). In the absence of any applied mechanical stimulation, the total infected area, was reduced by about 60 % when compared to normal fully actuated conditions (Figure 4C-D). The reintroduction of flow alone, did not significantly affect infection area when compared to non-mechanically stimulated conditions. In contrast, we observed that the application of stretching forces (peristalsis) significantly increased the efficiency of infection by approximately 50%, as reflected in the number and size of foci (Figure 4C, 4E). Although these results suggest that intestinal flow alone does not significantly increase *Shigella* infection area, they strongly suggest that it facilitates the bacterial multiplication (Figure 4B) and, moreover this was tightly controlled, since exposure to a faster flow rate inhibited the invasion dramatically (Figure S1E) (about 90%).

Overall, our results show that recreation of the architecture and mechanical forces of the intestine strongly impact several stages of *Shigella* infection. First, the bacterial adhesion is favored by the tissue architecture in 3D, enabling a strong T3SS activation once bacteria reach crypt-like areas of the colonic epithelia. Then, bacterial invasion from the apical side of the epithelium is strongly boosted by peristaltic motion and finally, the propagation is further facilitated upon physiologically relevant sheer stress created by flow.

Discussion

Historically, the Transwell™ system and polarized Caco-2 epithelial cells have been extensively used for studying *Shigella* infection *in vitro*. While enterocytes are the major cell type of the intestinal epithelium, invasion of cells from the apical side of epithelial monolayer cultured on Transwell™ has been surprisingly inefficient (Mounier et al., 1992). However, clinical data have been reported showing that only a few hundred to a few thousands of bacteria were sufficient to cause diarrheal symptoms (DuPont et al., 1989). Since *Shigella* invades M cells *in vivo* (Sansonetti et al., 1996), the following dogmatic model has thus been proposed: *Shigella* invades initially the epithelium through M cells from the Peyer's patch and subsequently invade adjacent enterocytes by basolateral spreading. In the present study, we observed that *Shigella* could also invade directly and very efficiently when applied via the luminal side of the intestinal epithelium composed solely of enterocytes, assuming cells are cultured in 3D *in vivo*-relevant microenvironment. While the 3D maturation of the epithelial layer exposed to mechanical forces is known to induce changes in Caco-2 transcriptome (Kim et al., 2016), Caco2 cells culture on -Chip does not lead to M cells differentiation, as one of their specific marker GP2 is not detected on-chip (Kim et al., 2016). Therefore, our results underscore the existence of multiple cellular routes employed also by *Shigella* to invade successfully the intestinal epithelium and indicate that the M-cell model is not exclusive. With the current studies we provide strong evidence on the importance of the previously

unappreciated role of the microenvironment, including 3D tissue architecture and mechanical forces, in *S. flexneri* infection. Our data suggest that the organization of the epithelial monolayer in developing 3D crypt-like structures provides a safe niche that is very important in protecting bacteria against luminal flow and thus, enabling their adhesion and subsequent activation of the T3SS. Further, our data uncover the contribution of peristalsis, as it greatly enhanced *Shigella* invasion. This result might reflect change in their deposited ECM, affecting the stiffness of the membrane and/or relaxation of the intercellular junctions, by stretching forces, thereby rendering the epithelium more permissive to the invasion process. It will be important in the future to determine the exact mechanism by which stretching forces modulate *Shigella* infection.

Over the years, many models have been developed to study *Shigella* infection. On one hand, small animal models have been tremendously helpful to understand the pathogenicity *in vivo* (Arena et al., 2015; Sansonetti et al., 1996). On the other hand, standard 2D *in vitro* culture systems contributed to uncover the molecular mechanisms of infection. Recently, enteroids and stem cells culture emerged also as a promising model by providing a more faithful and precise 3D environment *in vitro* (Dutta and Clevers, 2017)(Ranganathan et al I&I 2019, Koestler et al, I&I 2019). While each of these models comes with inherent advantages, all have important limitations in uncovering the effects of physical forces, the tissue is exposed to *in vivo*. Since a variety of forces are exerted at the intestinal interface in both physiological and disease states, employing new *in vitro* models for interrogating the role of biophysical forces in host-pathogen interactions is necessary. Here, we show that the technology of bioengineered microphysiological systems, as provided by Organ Chips carries this potential, together with the associated reduction in use of small animals for experimentation. Organ-Chips affords the physiological relevant architecture, mechanical forces, and microenvironment. While the advantages of this technology have been shown in drug safety

and efficacy testing (Foster et al., 2019), we show here that this model could also be powerful for investigating infection due to human restricted pathogens and even more, to provide new insights in this process in a very controlled manner. Thus, the Intestine-Chip model opens new avenues for biomedical research of host pathogens interactions in a more physiological environment.

Acknowledgements

The authors would like to thank Maryse Moya-Nilges and Jacomine Krijnse Locker from the Unité de Bio-imagerie ultra-structurale of Institut Pasteur. We also thank Héloïse Mary from the Biomaterials and Microfluidics core facility and P.H. Commere from the flow cytometry facility of Institut Pasteur. We would also like to thank Jacob P. Fraser from Emulate, Inc. for the initial training on the platform. We also thank P. Brodin, M. Ferrari and FX Campbell-Valois for comments and discussion on the manuscript. AG was supported by a Roux fellowship from Institut Pasteur, the PTR22-2016 from the Institut Pasteur, the Institut Carnot Pasteur MS and ANR-17-CE15-0012-01.

Figure legends

Figure 1. (A) A photograph of the Intestine-Chip. Scale bar represents 1 cm. (B) Scheme of a frontal plane of an Intestine-Chip central channels. Upper channel is blue and lower channel is pink. Lateral arrows represent lateral stretching by the side chambers (C) Stitched images showing intestinal protrusions from a frontal cross sectioning. Slices were acquired on a swept confocal microscope and Z projected. Cells were fixed, permeabilized and stained for actin (phalloidin-Alexa647, blue), with anti villin-1 (green) and nuclei with DAPI (red). (D) Representative view of a *Shigella*-WT-GFP infected chip after 60 minutes of bacterial exposure (Top) or polystyrene beads coated with AlexaFluor-350 (Bottom). Merge (left), zoom from merge (middle) and zoom of GFP fluorescence or AlexaFluor-350 (right) images are shown. Scale bar represents 100 μ m. (E) Stitched images showing a cross sectioning of an intestine-Chip infected by *Shigella*-WT-GFP (green) for one hour. Nuclei were stained with Dapi (red). (F) Quantification of *Shigella*-WT-GFP distribution within crypt or villi structures from cross sectioning images of epithelium grown in Intestine-Chip (n=8). Unpaired Student's *t* test, P***, P< 0.0001. (G) Representative scanning electron microscopy images of epithelium grown in an Intestine-Chip. A magnification of the white dotted area (left) is shown on the right. (H) Representative scanning electron microscopy images of epithelium grown in a Intestine-Chip and challenged with *Shigella*-WT-GFP infected chip for 1 hour. A magnification of the white dotted area (left) is shown on the right. (I) Quantification of *Shigella*-WT (left, N=40) and polystyrene beads (right, N= 23) distribution within Crypt or villi from SEM images. Intestine-Chips were infected for one hour. (J) Representative images of Intestine-Chip uninfected (left), infected by *Shigella*-WT-GFP (middle), infected by *Shigella*-*mxiD*-GFP. Brightfield (Top), GFP fluorescent (middle) and merged (Bottom) images. Infection was performed overnight (K) Frontal cross sections of uninfected control (left) and *Shigella*-WT-GFP (green) infected chips (right). Brightfield (top), GFP fluorescent

(middle) and merged (bottom) images. Infection was performed overnight. Scale bar represents 100 μm . (L) Quantification of *Shigella*-WT-GFP and *Shigella-mxiD*-GFP surface occupancy. Area of all detected individual GFP spots from 15 fields of view from a representative chip are shown, mean \pm SD, n= 135 for *Shigella*-WT-GFP and n= 633 for *Shigella-mxiD*-GFP. Unpaired Student's *t* test, P***, P< 0.0001. (M) Quantification of epithelial villi-like structures height (mean \pm SD, uninfected n=53 from 4 different slices, *Shigella*-WT-GFP n=76 from 5 different slices). Unpaired Student's *t* test, P***, P< 0.0001.

Figure 2. (A) Top view of chips infected overnight with *Shigella*-WT-GFP (green). Before infection, Caco-2 cells were cultured for 2 days (flat -2D) epithelium (Top) or for 6 days (3D epithelium) (Bottom). Brightfield (Left), GFP fluorescent (middle) and merge (right) images are shown. Scale bar represents 100 μm . (B) Quantification of epithelium infection by *Shigella*. Epithelium were grown in Intestine-Chip or Transwell and infected apically for 2 hours using MOIs of 1 and 100. As a control, infection of *Shigella-mxiD* was performed at a MOI of 100. Then, extracellular bacteria were removed by washes and one-hour gentamicin treatment. *Shigella* were collected by epithelium lysis and CFU were determined by plating dilution series of lysates. Data represents mean of n=2 for Intestine-chip and n=3 for each conditions of Transwell. Errors bars represents S.E.M and statistics were performed using an one-way ANOVA with Bonferroni's multiple comparison test, P***, P< 0.0001 (C) Representative images of a Intestine-Chip matured for 6 days under intestinal physiological conditions and infected for 2 hours with *Shigella* WT-GFP inoculum of 100,000 colony forming units (CFU)(left), 10,000 CFU (middle left), 1,000 CFU (middle right) or 100 CFU (right) before replacement of cell culture media supplemented with gentamicin overnight. Brightfield (Top), GFP fluorescent (middle) and merge (Bottom) images are shown. Scale bar represents 100 μm . (D) Quantification of *Shigella* WT-GFP infection area by

immunofluorescence. Index represents the total surface of detected foci per condition divided by the sum of total surface of all conditions. Results are cumulative from 2 separate experiments. (E) Representative images of time-lapse live imaging of Intestine-Chip infected by *Shigella* WT-GFP. Events detected in the upper channel (Top) and in the lower channel (Bottom) are shown after 30 min (Left), 2 hours (middle left), 6 hours (middle right) and 15 hours (right). Scale bar represents 100 μ m. (F) Quantification of the number of bacteria detected per foci over time in the upper channel (green) and lower channel (pink), n= 16 foci.

Figure 3. (A) Stitched images showing cross sections of epithelium grown in 3D (Top) or 2D (Bottom) in Intestine-Chip and infected for one hour (adhesion step) by *Shigella*-WT-mcherry (Red) expressing the fluorescent reporter TSAR (green) . Nuclei were stained with Dapi (red). (B) Quantification of *Shigella* adhesion by CFU counting. No significant differences were observed between different conditions using one-way ANOVA with multiple comparisons test. (C) Quantification of the percentage of the number of activated bacteria detected by TSAR (green) relative to the total number of bacteria (Red) after one hour of infection in epithelium grown in 3D or 2D in Intestine-Chip under application of mechanical forces. Data represents the mean +/- SD of 2 chips from 2 independent experiments. Statistics were performed using an one-way ANOVA with multiple comparisons test. *, P< 0.01 (D) Stitched images showing cross sections of epithelium grown in 3D (Top) or 2D (Bottom) in Intestine-Chip and infected for 3 hours (invasion step) by *Shigella*-WT-mcherry (Red) expressing the fluorescent reporter TSAR (green) . Nuclei were stained with Dapi (red). (E) Quantification of *Shigella* invasion by CFU counting. Data represents the mean +/- SD of 2 chips from 2 independent experiments. Statistics were performed using an one-way ANOVA with multiple comparisons test. ****, P< 0.00001.

Figure 4. (A) Stitched images showing cross sections of epithelium grown in 3D (Top) or 2D (Bottom) in Intestine-Chip and infected for 15 hours (propagation step) by *Shigella*-WT-mcherry (Red) expressing the fluorescent reporter TSAR (green) . Nuclei were stained with Dapi (red). (B) Quantification of *Shigella* propagation by CFU counting. Data represents the mean +/- SD of 2 chips from 2 independent experiments. Statistics were performed using an one-way ANOVA with multiple comparisons test. **, P< 0.001 and ***, P< 0.0001. (C) Representative images of *Shigella* WT-GFP infected Intestine-Chip under no flow and no peristalsis (left), flow only (middle left), peristalsis only (middle right) or under both flow and peristalsis (right). Brightfied (top), GFP fluorescent (middle) and merge (bottom) images are shown. Chips were infected overnight with cell culture supplemented with gentamicin 2 hours after bacterial addition. Scale bar represents 100 μm (D) Quantification of *Shigella* WT-GFP foci spreading for each condition (No Flow/No stretch, Flow only, Stretch only, Flow and Stretch). Results are expressed as an index representing the total surface of detected foci for each condition divided by the sum of all conditions. Mean +/- SD, n=242, 79, 337 and 580 respectively from 28-62 fields of view and 2-5 independent experiments were performed. An analysis of variance (ANOVA) was used with Bonferroni's post test , ** P< 0.005. (E) Quantification of infection index relative to the number of foci. Mean +/- SD of 2-5 independent. N=242, 79, 337 and 580 foci respectively from 28-62 fields of view experiments were performed. An analysis of variance (ANOVA) was used with Bonferroni's post test, P*, P< 0.05.

Supplementary Figure 1. (A) Maturation of Caco-2 cells cultured in the Intestine-Chip under flow (30 μL /hour) and peristalsis (10%, 0.15 Hz). On day 1, Chips were activated, coated with ECM and Caco-3 cells were seeded. On day 2, adherent Caco-2 reached 100% confluence on the porous membrane . On day 6, protrusions were clearly visible on

brightfield. Scale bar represents 100 μm (B) Representative top view image of an epithelium matured on the Intestine-Chip (Left). Image is generated by stitching multiple Z-series and Z projected. Caco-2 cells were gene-edited for expressing E-Cadherin-GFP (green). After fixation in PFA, nuclei were stained using Dapi (Red) and the actin cytoskeleton was stained using phalloidin-Alexa-647 (Blue). A 3D reconstruction of a section highlighted by a white square on the left is shown on the right. (C) Representative images of 200 μm vertical cross sectioning of Intestine-Chip matured for 6 days. Pictures represent stitched images acquired on a swept confocal using an 20x air objective. Cells were fixed, permeabilized, and immunostained with (Left) anti-Fabp1 (green) and corresponding secondary antibody, F-actin was stained with phalloidin-Alexa555 (red) and nuclei were stained with DAPI (blue); (Right): using anti-Krt-20 (green) and corresponding secondary antibody, F-actin was stained with phalloidin-Alexa555 (red) and nuclei were stained with DAPI (blue). (D) Permeability of the epithelium was determined in overnight infected (n=2) and non-infected Intestine-Chip (n=4) by measuring the apparent permeability of 70kD Dextran-FITC diffusing from the upper to lower channel after overnight perfusion (1mg/ml). As a control, permeability was also assessed using empty Intestine-Chip (n=3). About 70 % leakage was observed. (E) Images of uninfected (Top) and *Shigella*-WT-GFP overnight infected Intestine-Chip under stretching and two flow rate regimes: 30 μL /hour (middle) and 400 μL /hour (bottom). GFP fluorescent (Left), Brightfield (middle) and merged (Right) are shown. Scale bar represents 100 μm . (F) Quantification of infection of experiments shown in (E) representing the infected surface area measured in each condition.

Supplementary Figure 2. (A) Representative images of *Shigella* WT-GFP recruitment over time within 3D epithelium cultured in an Intestine-Chip. Brightfield (top) and fluorescent (middle) images were acquired at 30 min (left), 60 min (middle) and 120 min (right). An

overlaid image is shown at the bottom. Scale bar represents 100 μm (B). Representative image of *Shigella* WT-GFP (green) foci and counterstained against LPS (Red) Nuclei are stained with Dapi. Intestine-Chip was infected overnight with gentamycin protection. A merged image is shown with phalloidin staining (white). Scale bar represents 100 μm (C) Representative images of infection of wild-type *Shigella*-WT-GFP (green) of Caco-2 cells grown on TranswellTM. Transwell was infected overnight with gentamycin protection. Extracellular bacteria were counterstained using anti-LPS (red). Nuclei were stain with DAPI (Blue) and actin stained with phalloidin-Alexa647 (purple). Scale bar represents 20 μm .

Supplementary Figure 3. (A) Stitched images showing cross sections of epithelium grown in 3D and infected for 1 hour with *Shigella*-WT-mcherry-TSAR (top) or *Shigella-icsA*-GFP (middle) or *Shigella-mxiD*-GFP (bottom). (B) Quantification of *Shigella* infection by CFU counting. Intestine-Chips were infected for one hour. Data represents the mean \pm SD of 2 chips from 2 independent experiments. Statistics were performed using an one-way ANOVA with multiple comparisons test. *, $P < 0.01$. (C) Representative images of *Shigella-icsA* -GFP infected Intestine-Chip. (Top) Top viewed of the infected Intestine-Chip. Brightfield (Left), GFP fluorescent (middle left), merged (middle right) and zoom (Right) images. Zoom image corresponds to the white dotted box shown in merged image. (Bottom) Cross-section of *Shigella-icsA* -GFP infected Intestine-Chip. Sections were immunostained using anti-LPS (middle-red), merged image is shown on the right. White arrow shows *Shigella-icsA* -GFP that do not colocalized with LPS (infected cell). Yellow arrow shows *Shigella-icsA* -GFP colocalizing with LPS (external bacteria). Intestine-Chips were infected for one hour. Scale bars represent 100 μm .

Supplementary Figure 4. (A) Representative images of time-lapse live imaging of Intestine-Chip infected by *Shigella* WT-mcherry (red) with 1 μm fluorescent beads (blue). Events

detected in the upper channel (Top) and in the lower channel (Bottom) are shown after 30 min (Left) and 15 hours (right). Scale bar represents 100 μ m. (B) Representative image of cell viability within infection foci using Draq7 marker (purple). This dye only stains the nuclei in dead and permeabilized cells. Time of infection shown corresponds to 15 hours. (C) Representative images of Intestine-Chip infected for 2 hours by *Shigella*-WT (Red) in which epithelium was disrupted upon EGTA treatment (Bottom) or not as a control (Top). Cells were fixed and stained for ZO-1 (green) by immunolabelling and for actin using phalloidin-Alexa-350 (Blue). Nuclei were stained with DAPI (Blue). (D) Quantification by CFU counting of *Shigella*-WT invasion in control and in EGTA disruption conditions (n=2).. Results are expressed as a ratio of CFU as compared to control condition.

Supplementary movie 1: Z stacks of images showing intestinal protrusions using Intestine-Chip and acquired on a swept confocal microscope. Caco-2 cells gene-edited for expressing E-Cadherin-GFP (green) were grown for 6 days on Intestine-Chip, then cells were fixed, permeabilized and stained for actin (phalloidin-Alexa647, blue) and nuclei with DAPI (red).

Supplementary movie 2: Representative movie of 3D matured Caco-2 cells on Intestine-Chip infected at the apical side with *Shigella* WT-GFP at MOI 0.1 for up to 15 hours. Imaging of the top channel is shown on the left and imaging of the bottom channel is shown on the right of the infected chip. Images were acquired every 15 min.

Materials and Methods

Cell culture and bacterial strains

Caco-2 cells (clone TC-7) were obtained from ATCC. Cells were grown in Dulbecco's Modified Eagle Medium (DMEM, Gibco) supplemented with 20 % FBS (fetal bovine serum, Biowest) and non-essential amino acid (Gibco) in 10% CO₂ at 37°C.

The wild type derivative *Shigella flexneri* 5a (M90T) (Sansone et al., 1982), the *mxiD* mutant derivative of the wild type strain (Allaoui et al., 1993) and the *icsA* mutant derivative of the wild type strain (Bernardini et al., 1989) were used. All these strains harbor the pFPV25.1 plasmid encoding GFPmut3. TSAR plasmid was described previously (Campbell-Valois et al., 2014; 2015). Bacteria were grown at 37°C on trypticase soy (TCS; Becton Dickinson) agar plates containing 0.01 Congo red (Serva). Individual colonies were grown at 30°C overnight with ampicillin. From this culture, bacteria were grown at 37°C in TCS to obtain a suspension of 10¹⁰ CFU/mL.

Human Intestine-Chip

Intestine-Chips made of polydimethylsiloxane (PDMS) and associated instrumentation and software (Human Emulation System) for culturing the chips were obtained from Emulate, Inc. (Boston, MA).

Chips were activated for ECM coating per manufacturer instructions. Briefly, chips were rinsed in 70% ethanol (Sigma-Aldrich) followed by sterile water (Gibco) and ER-2 solution (Emulate). Then, chips were activated using ER-1 solution (Emulate) and exposed for 20 min under UV light (36W, 365nm). Finally, chips were rinsed with ER-2 solution followed by PBS (Gibco). Then, ECM coating was performed by incubating an ECM solution (100mg/mL of Matrigel (Corning) and 30 ug/mL rat tail Collagen type 1 (Gibco) diluted in DMEM

(Gibco)) for 2 hours at 37°C 5% CO₂. Cells were seeded at a concentration of 1.5 millions/mL in the upper channel for 2 hours at 37°C 5% CO₂. After cell attachment, upper channel was gently washed using warm cell culture media supplemented with 100U/mL penicillin and 100ug/mL streptomycin. Cells were maintained statically overnight. Then, chips were connected to the instrument (Emulate) and maintained for the duration of the culture. The following cell culture conditions were applied: 37°C, 5% CO₂, flow at 30uL/h and 10% of lateral mechanical stretching at a frequency of 0.15 Hz. Cell culture media was equilibrated and refreshed every 48 hours.

Intestine-Chip infection

Intestine-Chips were washed overnight at 30uL/hour in regular cell culture media without penicillin and streptomycin in both channels. Then, *S. flexneri* (neither coated with poly-L-lysine nor expressing exogenous adhesin) were introduced in the top channel from the Pod reservoir. To synchronize the exposure of bacteria over the full surface of the top channel, a fast flow of 400uL/hour for 30 min was performed. The end of this pulse corresponds to time zero. Then, flow and/or stretching conditions were applied for the duration of the experimental condition. To determine the adhesion capacity, infection duration was one hour. At this end of this challenge, chips were washed twice with regular cell culture media using gravity flow. Bacteria were recovered using 0.5 % sodium deoxycholate (Sigma-Aldrich) and diluted lysate series were plated with ampicillin. For immunofluorescence, chips were removed from the instrument at the end of the incubation time and infection was stopped by gently flushing 4% of paraformaldehyde (Electron Microscopy Sciences) diluted in PBS with Ca²⁺ and Mg²⁺ (Gibco) in top and bottom channels.

To determine invasion capacity, infection duration was three hours as follow: after a 2 hours challenge, extracellular bacteria were washed at 400uL/hour for 30 min in cell culture media

supplemented with gentamycin at a final concentration of 50ug/mL (ThermoFisher). Then, Intestine-Chip were incubated for an additional 30 min under their mechanical conditions prior bacteria recovery or immunofluorescence processing as described previously. To determine propagation capacity, infection duration was 15 hours as follow: after 2 hours challenge, Intestine-Chip were washed at 400uL/hour for 30 min in cell culture media supplemented with gentamycin at a final concentration of 50ug/mL (ThermoFisher). Then, chips were incubated for 12h30 under their mechanical conditions prior bacteria recovery or immunofluorescence processing as described previously.

For EGTA disruption, Intestine-Chip were briefly rinsed with Calcium free ringer buffer supplemented with 100mM EGTA. Then, infection were performed using this buffer as described for the invasion step assay.

For beads distribution assay, blue fluorescent microspheres (FluoSpheres carboxylate-modified, F8815, Invitrogen), of a diameter of 1um were used at a concentration of 1 million/mL under the same experimental settings as *Shigella* infection.

Transwell infection

Caco-2/TC7 cells, 2×10^5 cells/cm² cells were seeded into 12-well or 6-well Transwell inserts (pore size 0.4 μ m, Corning) and cultured for 18-21 days at 10% CO₂ at 37° C; fresh media was added triweekly. *S. flexneri* (neither coated with poly-L-lysine nor expressing exogenous adhesin) were pelleted, washed with PBS and resuspended in infection medium to MOI 1 or 100. Apical and basal chambers were washed twice with warm DMEM-Hepes and bacteria were added to the apical chamber, incubated for 2 hours at 37 °C in CO₂ incubator and then apical/basal medium was aspirated and replaced for fresh DMEM-Hepes supplemented with gentamicin 50 μ g/mL and incubated for 1 hour at 37 °C in CO₂ incubator before recovering

bacteria using 0.5 % sodium deoxycholate (Sigma-Aldrich) and plated dilution on ampicillin plates.

Immunofluorescence

Chips were fixed in 4% of paraformaldehyde (Electron Microscopy Sciences) diluted in PBS with Ca²⁺ and Mg²⁺ (Gibco) for 30 min. Top and bottom channels were flushed with PBS after fixation. If the immunostaining was not performed immediately, chips were immersed in cold PBS and stored at 4°C. For transversal sections, chips were cut in 200um thick slices using a vibrating blade microtome (VT1000S, Leica). Sections were permeabilized in buffer A (PBS/0.2% Triton X-100/ 0.5% BSA) for 1 hour at room temperature (RT) and incubated with primary antibody diluted in buffer A supplemented with 1% DMSO for 2 hours at RT or overnight at 4°C. Primary antibodies used were:

Antigen	Dilution	Catalogue #	Isotype	Manufacturer
Villin 1	1:200	610358	Mouse IgG ₁	BD Biosciences
Villin 1	1 :100	Ab739	Mouse	Abcam
FABP1	1:200	hpa028275	Rabbit	Sigma-Aldrich
Krt20	1:200	M7019	Mouse IgG	Dako
LPS	1:300	in house	Rabbit	in house
ZO-1	1 :100	617300	Rabbit	Invitrogen

Then, chip sections were washed at least 3 times in buffer A for 15 min and stained for 2 hours at RT with secondary antibodies Alexa Fluor A568 or Fluorescein isothiocyanate (FITC) goat anti-mouse or anti-rabbit (Life technologies). Staining with wheat germ agglutinin Alexa Fluor A555 (no. W32464, Life technologies), DAPI (Life technologies) and phalloidin Alexa Fluor A350 or A647 (Life technologies) were performed for 1 hour at RT in

Buffer A. Samples were rinsed at least 3 times in PBS and imaged immediately and directly in PBS on coverslips #1.5 (Corning and Matek).

Light Microscopy

Chips under maturation were observed on an automated microscope (Zeiss, Axio observer Z1) equipped with Colibri 2 and camera (Orcaflash 4 v2.0, Hamamatsu). A full scan of the upper channel was performed with a 10x air objective (Zeiss Plan Apochromat 10x 0.45 N.A) in brightfield. Z-series of optical sections was photographed from the porous membrane to the top of the tissue. For infection experiments, a full scan of the upper channel was performed using the 10x objective. This allows capturing all locations of foci of infection of GFP-expressing *S. flexneri*. Exposure time was about 200ms. Regions of interest were also acquired with a 20x air objective (Zeiss Plan Neofluor 20x 0.4 N.A). Sections between 200um and 300um-thick were imaged using an Opterra swept confocal microscope (Brucker) mounted on a Zeiss axio observer Z1 and equipped with an EMCCD Evolve 512 Delta camera (Photometrics). Exposure time was about 100-200ms using an EM gain of about 550. Live cell imaging was performed in an environmental control system set to 37°C and 5 % CO₂. Nemesys low-pressure modules (Cetoni) and pressure controller OB-1 MkIII+ (Elveflow) were used for controlling flow and stretching conditions. Microscopy images were adjusted for brightness, color balance, and/or contrast uniformly across all pixels, as necessary, in image J (v1.46r, National Institutes of Health) or ICY Software (Institut Pasteur).

Fluorescent image analysis

To quantify the infection efficiency based on fluorescence images, borders of foci of infection were visually detected and regions of interest (ROI) were hand-drawn using ImageJ. A foci is

defined as a surface area infected by *Shigella*. Then, two parameters were measured : the number of detected foci and the area of these detected individual foci. Results are expressed as an index of infection relative either to the number of foci or the surface area of foci. Index of infection is calculated as the total number detected foci for each condition divided by the sum of all.

To quantify the distribution of *Shigella* into crypt or villi like structure from Intestine-Chip sections, we define ROIs corresponding to villi and crypt and used ICY software (<http://icy.bioimageanalysis.org>) Spot Detector plugin that allow for an automatic bacteria detection. To assess for TSAR activation during the adhesion time-point, the Intestine-Chips were infected with TSAR producing strain for 1 hour. This strain expresses constitutively mCherry and upon T3SS induction also express GFP. After fixation, sections of Intestine-Chips were imaged using an Opterra swept confocal microscope and analysed with ICY software plugins. We used Spot Detector plugin to automatically detect objects corresponding to red and green bacteria (mCherry and GFP) and then we used Colocalization Studio plugin (method: object based and statistical colocalisation, SODA (Lagache et al., 2018), to quantify the number of mCherry bacteria producing GFP, hence TSAR activated.

Scanning electron microscopy

Cells were fixed in 2.5 % glutaraldehyde in PHEM buffer (pH 7.0) for 1 hour at RT and washed 3x 5min in distilled H₂O. The top of the upper channel of the chip was open by successive longitudinal 900 µm thick slices using a vibrating blade microtome (VT1000S, Leica). Then, chips were post-fixed with 1% osmium tetroxide in distilled H₂O for 1h and rinsed with distilled H₂O . Cells were then dehydrated through a graded ethanol series (25, 50, 75, 95 and 100 %) followed by critical point drying with a Leica EM CPD 300. Finally dried specimens were sputter coated with a 10 nm gold/palladium conductive layer using a

gun ionic evaporator PEC 682. Images were acquired on a JEOL JSM 6700F field emission scanning electron microscope operated at 7kV. Quantification of *Shigella* and beads distribution within crypt and villi structures were manually score in a binary manner (i.e. scored as 1 if at least one bacteria was visually detected in the image or zero if not)

Permeability and viability assays

Intestine-Chip were prepared as previously mentioned and maintained under flow (30uL/hour) and stretching conditions (10%, 0,15Hz) for 6 days. An empty Intestine-Chip was used as a control. Each chip was microscopically examined before the assay. FITC-dextran 10 or 70 kDa was briefly introduced to the reservoir of the top channel (10ug/mL) in cell culture media. A brief a pulse of 400 uL/hour for 30 min was used to synchronize all chips. The end of this pulse corresponds to time zero. After 2 hours to overnight incubation, samples from the top and bottom were collected and fluorescence was measured in a spectrofluorometer (Infinite M200Pro, Tecan, Switzerland) with excitation wavelength of 488 nm and an emission wavelength of 520 nm. Permeability assay were performed from 2 experiments, each of which included 3 different chips.

For live cell imaging experiments, 1um blue fluorescent microspheres were simultaneously added to cell culture media with *Shigella* at time 0 of infection. Cell membrane integrity was determined by adding directly the far-red fluorescent dye Draq7 (Ab109202, Abcam) in cell culture media at a final concentration of 3uM for at least 30 min at 37°C.

Statistical analyses

Statistical significance was determines using unpaired Student's *t* test. For multiple comparisons, analysis of variance (ANOVA) was used with Bonferroni's or Dunnett's post test. Statistics were completed using prism 7 (GraphPad, La Jolla, CA).

References

- Allaoui, A., Sansonetti, P.J., Parsot, C., 1993. MxiD, an outer membrane protein necessary for the secretion of the *Shigella flexneri* Ipa invasins. *Mol. Microbiol.* 7, 59–68.
- Arena, E.T., Campbell-Valois, F.-X., Tinevez, J.-Y., Nigro, G., Sachse, M., Moya-Nilges, M., Nothelfer, K., Marteyn, B., Shorte, S.L., Sansonetti, P.J., 2015. Bioimage analysis of *Shigella* infection reveals targeting of colonic crypts. *Proc. Natl. Acad. Sci. U.S.A.* 112, E3282–90. doi:10.1073/pnas.1509091112
- Ashida, H., Mimuro, H., Sasakawa, C., 2015. *Shigella* Manipulates Host Immune Responses by Delivering Effector Proteins with Specific Roles. *Front. Immunol.* 6, 110–12. doi:10.3389/fimmu.2015.00219
- Bernardini, M.L., Mounier, J., d'Hauteville, H., Coquis-Rondon, M., Sansonetti, P.J., 1989. Identification of *icsA*, a plasmid locus of *Shigella flexneri* that governs bacterial intra- and intercellular spread through interaction with F-actin. *Proc Natl Acad Sci USA* 86, 3867–3871.
- Brotcke Zumsteg, A., Goosmann, C., Brinkmann, V., Morona, R., Zychlinsky, A., 2014. *IcsA* is a *Shigella flexneri* adhesin regulated by the type III secretion system and required for pathogenesis. *Cell Host & Microbe* 15, 435–445. doi:10.1016/j.chom.2014.03.001
- Campbell-Valois, F.-X., Sachse, M., Sansonetti, P.J., Parsot, C., 2015. Escape of Actively Secreting *Shigella flexneri* from ATG8/LC3-Positive Vacuoles Formed during Cell-To-Cell Spread Is Facilitated by *IcsB* and *VirA*. *MBio* 6, e02567–14. doi:10.1128/mBio.02567-14
- Campbell-Valois, F.-X., Schnupf, P., Nigro, G., Sachse, M., Sansonetti, P.J., Parsot, C., 2014. A Fluorescent Reporter Reveals On/Off Regulation of the *Shigella* Type III Secretion Apparatus during Entry and Cell-to-Cell Spread. *Cell Host & Microbe* 15, 177–189. doi:http://dx.doi.org/10.1016/j.chom.2014.01.005
- Chaturvedi, L.S., Gayer, C.P., Marsh, H.M., Basson, M.D., 2008. Repetitive deformation activates Src-independent FAK-dependent ERK mitogenic signals in human Caco-2 intestinal epithelial cells. *Am J Physiol Cell Physiol* 294, C1350–61. doi:10.1152/ajpcell.00027.2008
- DuPont, H.L., Levine, M.M., Hornick, R.B., Formal, S.B., 1989. Inoculum size in shigellosis and implications for expected mode of transmission. *Journal of Infectious Diseases* 159, 1126–1128.
- Dutta, D., Clevers, H., 2017. Organoid culture systems to study host-pathogen interactions. *Current Opinion in Immunology* 48, 15–22. doi:10.1016/j.coi.2017.07.012
- Ferrari, M.L., Sansonetti, P.J., 2016. Cellular Invasion by Bacterial Pathogens, in: Bradshaw, R.A., Stahl, P.D. (Eds.), *Encyclopedia of Cell Biology*. Academic Press, Waltham, pp. 784–793. doi:http://dx.doi.org/10.1016/B978-0-12-394447-4.20077-1
- Foster, A.J., Chouhan, B., Regan, S.L., Rollison, H., Amberntsson, S., Andersson, L.C., Srivastava, A., Darnell, M., Cairns, J., Lazic, S.E., Jang, K.-J., Petropoulos, D.B., Kodella, K., Rubins, J.E., Williams, D., Hamilton, G.A., Ewart, L., Morgan, P., 2019. Integrated in vitro models for hepatic safety and metabolism: evaluation of a human Liver-Chip and liver spheroid. *Arch Toxicol* 93, 1021–1037. doi:10.1007/s00204-019-02427-4
- Gayer, C.P., Basson, M.D., 2009. The effects of mechanical forces on intestinal physiology and pathology. *Cellular signalling* 21, 1237–1244. doi:10.1016/j.cellsig.2009.02.011
- Kim, H.J., Huh, D., Hamilton, G., Ingber, D.E., 2012. Human gut-on-a-chip inhabited by microbial flora that experiences intestinal peristalsis-like motions and flow. *Lab Chip* 12,

- 2165–2174. doi:10.1039/c2lc40074j
- Kim, H.J., Ingber, D.E., 2013. Gut-on-a-Chip microenvironment induces human intestinal cells to undergo villus differentiation. *Integr. Biol.* 5, 1130–1140. doi:10.1039/C3IB40126J
- Kim, H.J., Li, H., Collins, J.J., Ingber, D.E., 2016. Contributions of microbiome and mechanical deformation to intestinal bacterial overgrowth and inflammation in a human gut-on-a-chip. *Proc Natl Acad Sci USA* 113, E7–E15. doi:10.1073/pnas.1522193112
- Koestler, B.J., Ward, C.M., Fisher, C.R., Rajan, A., Maresso, A.W., Payne, S.M., 2019. Human Intestinal Enteroids as a Model System of Shigella Pathogenesis. *Infection and immunity* 87. doi:10.1128/IAI.00733-18
- Kotloff, K.L., Nataro, J.P., Losonsky, G.A., Wasserman, S.S., Hale, T.L., Taylor, D.N., Sadoff, J.C., Levine, M.M., 1995. A modified Shigella volunteer challenge model in which the inoculum is administered with bicarbonate buffer: clinical experience and implications for Shigella infectivity. *Vaccine* 13, 1488–1494.
- Lagache, T., Grassart, A., Dallongeville, S., Faklaris, O., Sauvonnnet, N., Dufour, A., Danglot, L., Olivo-Marin, J.-C., 2018. Mapping molecular assemblies with fluorescence microscopy and object-based spatial statistics. *Nat Commun* 9, 698. doi:10.1038/s41467-018-03053-x
- Mounier, J., Vasselon, T., Hellio, R., Lesourd, M., Sansonetti, P.J., 1992. Shigella flexneri enters human colonic Caco-2 epithelial cells through the basolateral pole. *Infection and immunity* 60, 237–248.
- Parsot, C., 2009. Shigella type III secretion effectors: how, where, when, for what purposes? *Curr Opin Microbiol* 12, 110–116. doi:10.1016/j.mib.2008.12.002
- Ranganathan, S., Doucet, M., Grassel, C.L., Delaine-Elias, B., Zachos, N.C., Barry, E.M., 2019. Evaluating Shigella flexneri Pathogenesis in the Human Enteroid Model. *Infection and immunity* 87. doi:10.1128/IAI.00740-18
- Sansonetti, P.J., Arondel, J., Cantey, J.R., Prevost, M.C., Huerre, M., 1996. Infection of rabbit Peyer's patches by Shigella flexneri: effect of adhesive or invasive bacterial phenotypes on follicle-associated epithelium. *Infection and immunity* 64, 2752–2764.
- Sansonetti, P.J., Kopecko, D.J., Formal, S.B., 1982. Involvement of a plasmid in the invasive ability of Shigella flexneri. *Infection and immunity* 35, 852–860.
- Thomas, W.E., Trintchina, E., Forero, M., Vogel, V., Sokurenko, E.V., 2002. Bacterial Adhesion to Target Cells Enhanced by Shear Force. *Cell* 109, 913–923. doi:http://dx.doi.org/10.1016/S0092-8674(02)00796-1
- Womack, W.A., Barrowman, J.A., Graham, W.H., Benoit, J.N., Kvietys, P.R., Granger, D.N., 1987. Quantitative assessment of villous motility. *Am J Physiol* 252, G250–6. doi:10.1152/ajpgi.1987.252.2.G250

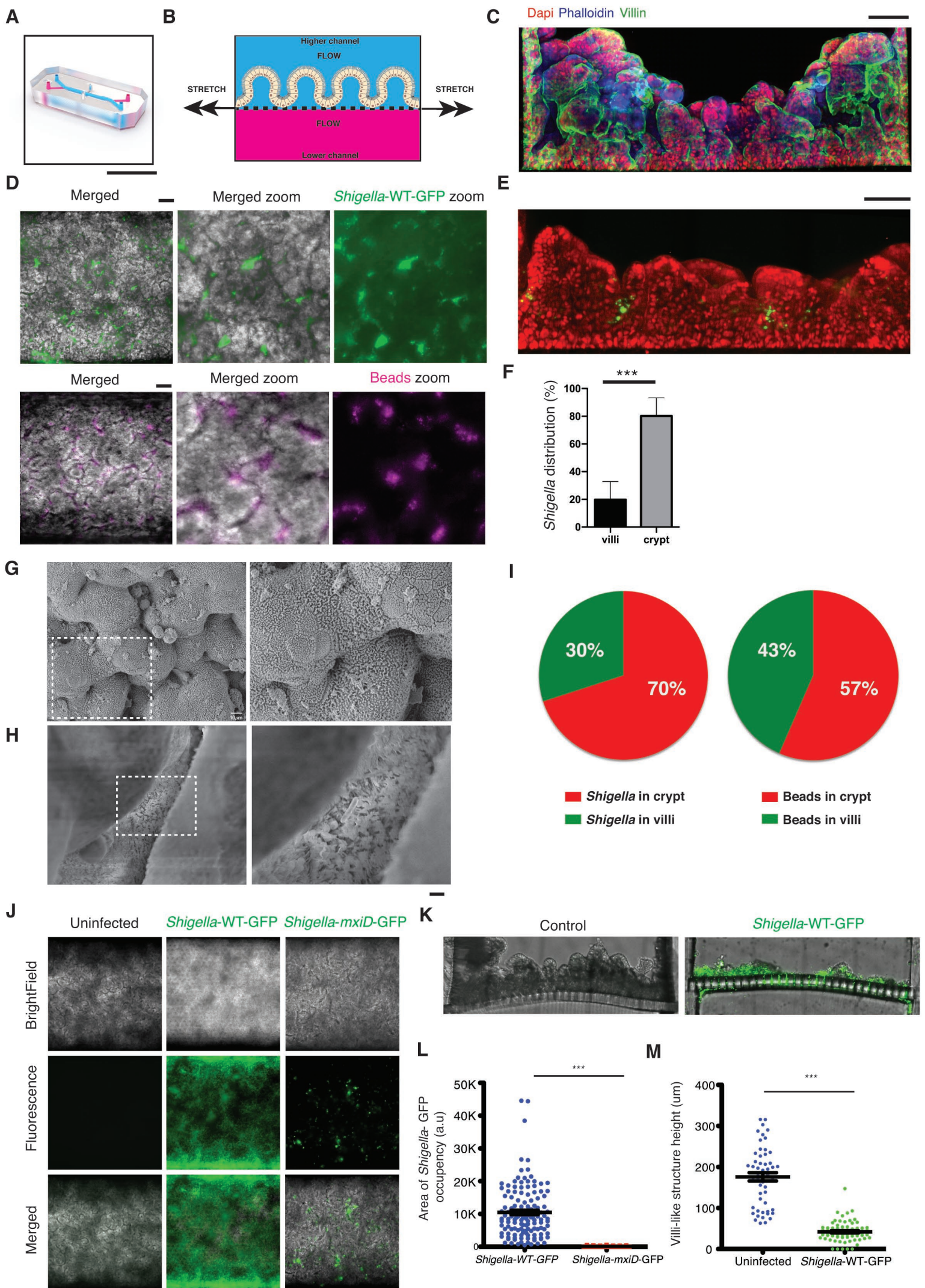


Figure 1

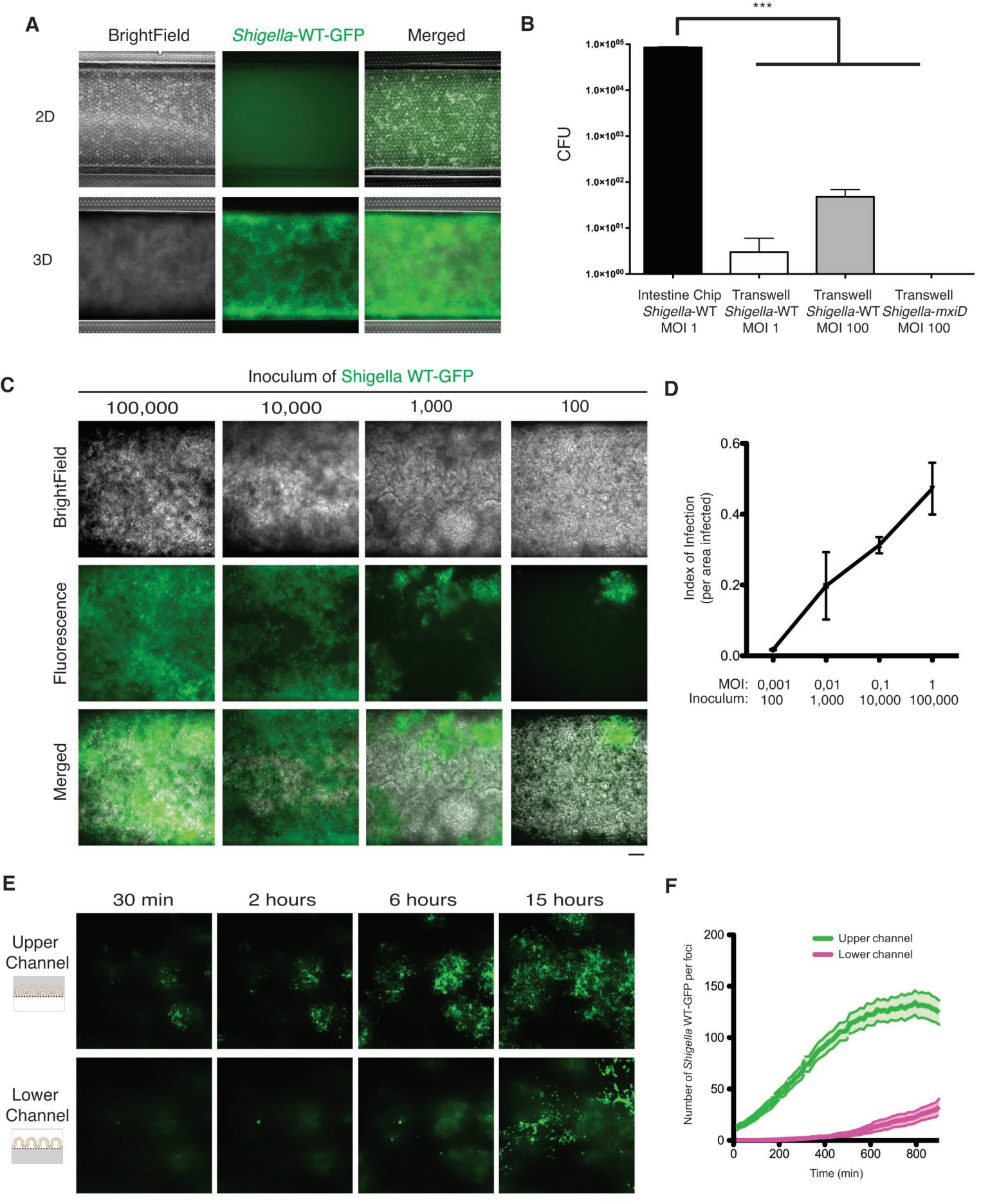
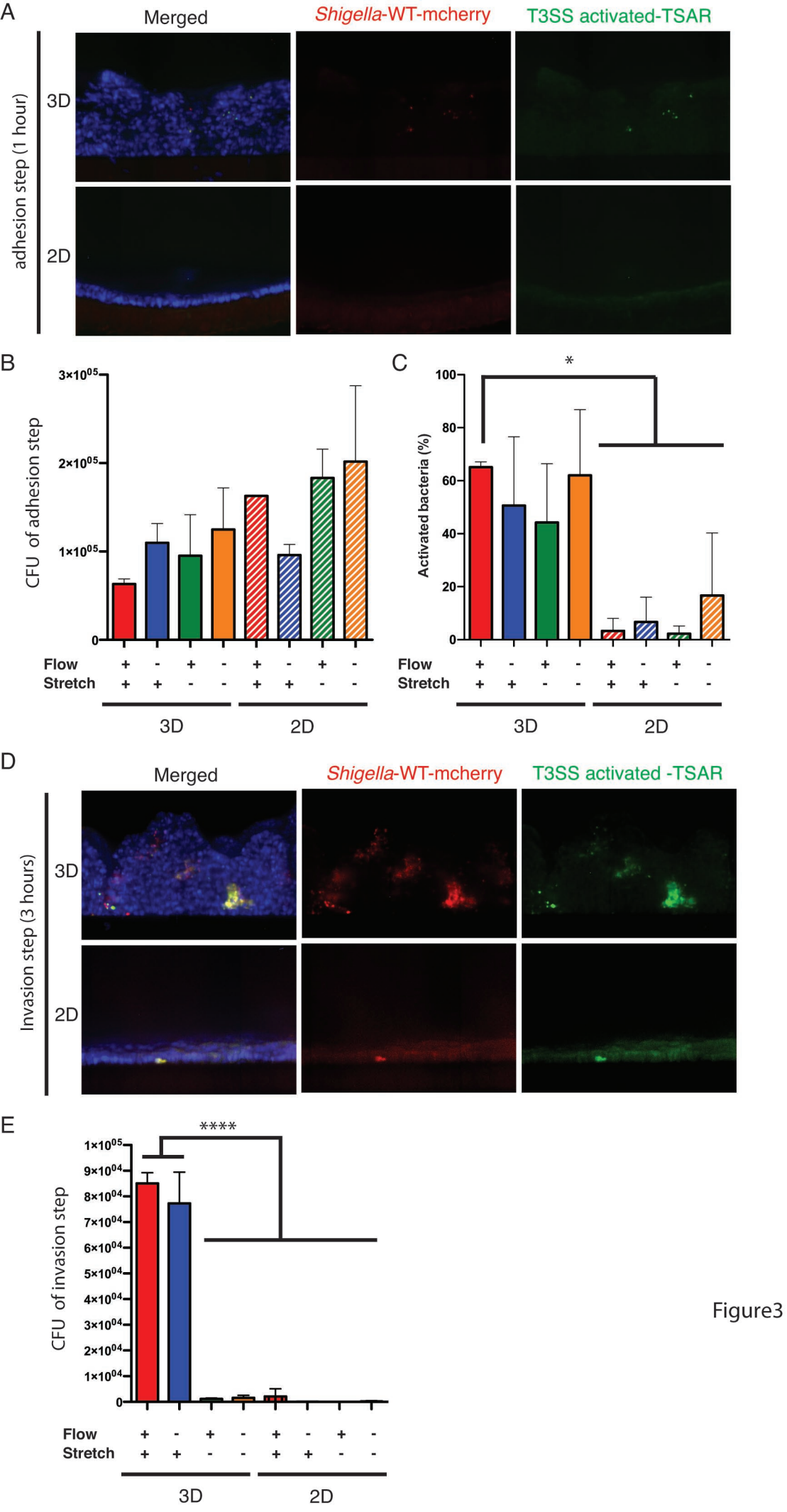


Figure 2



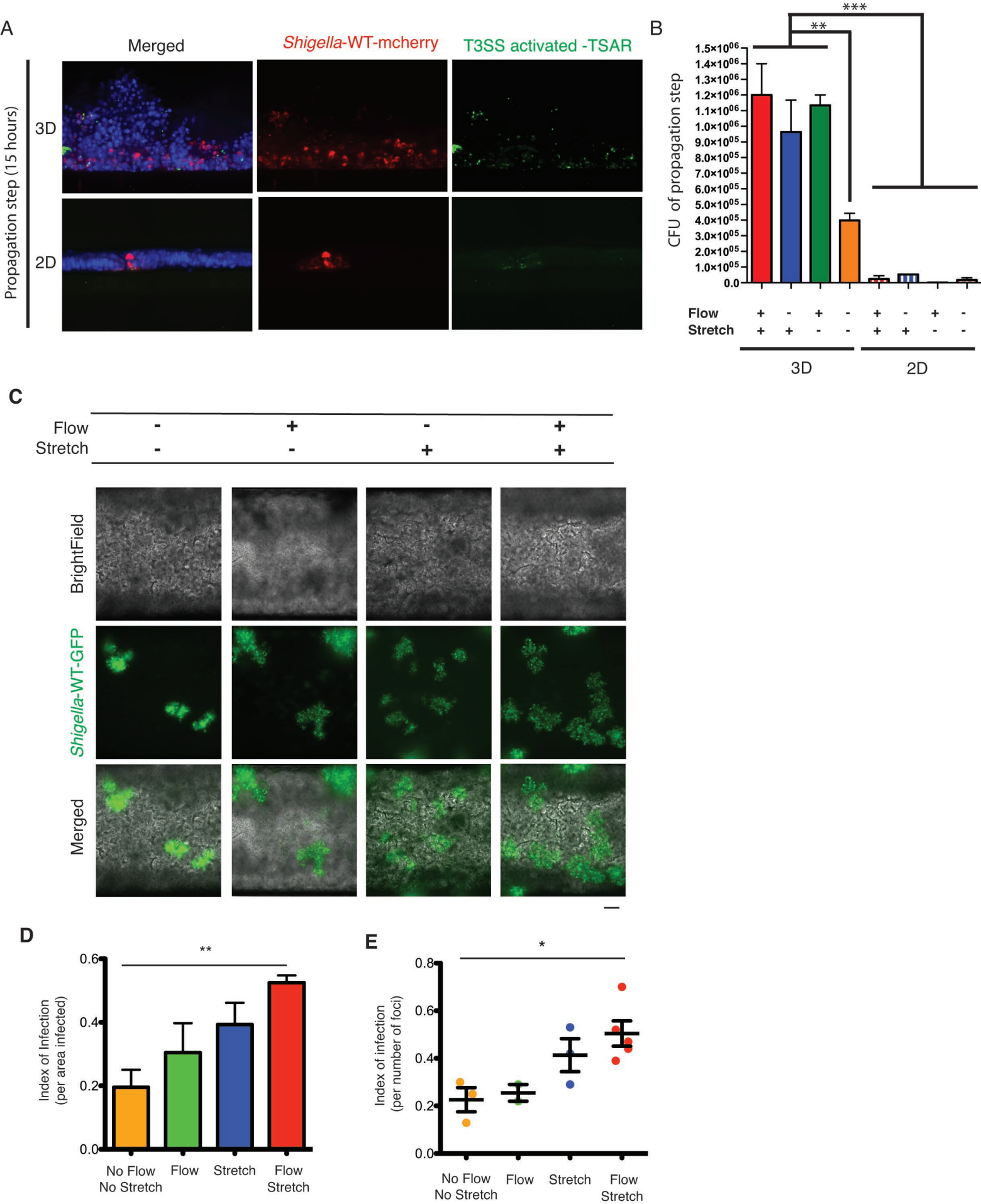
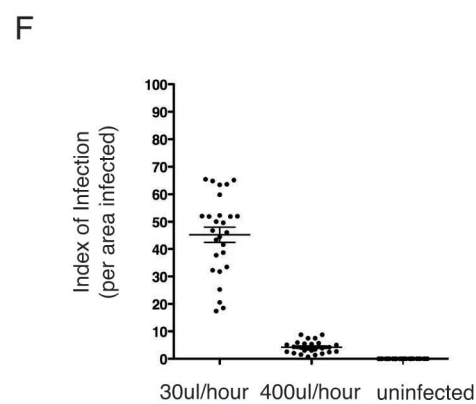
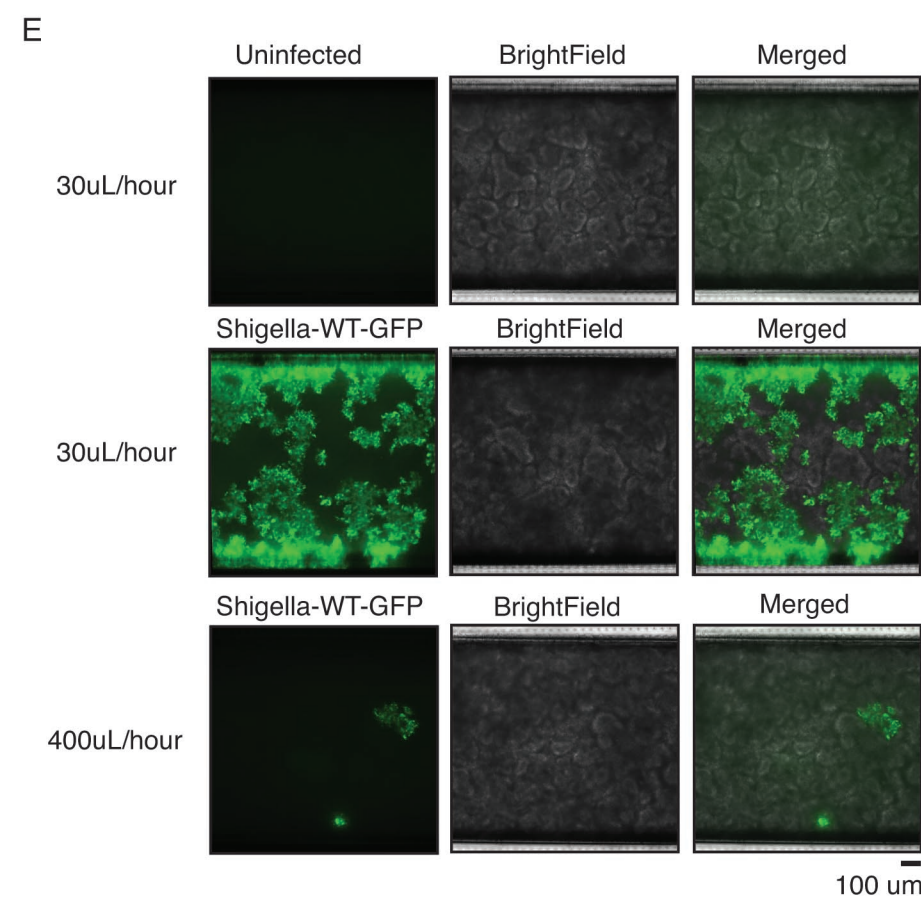
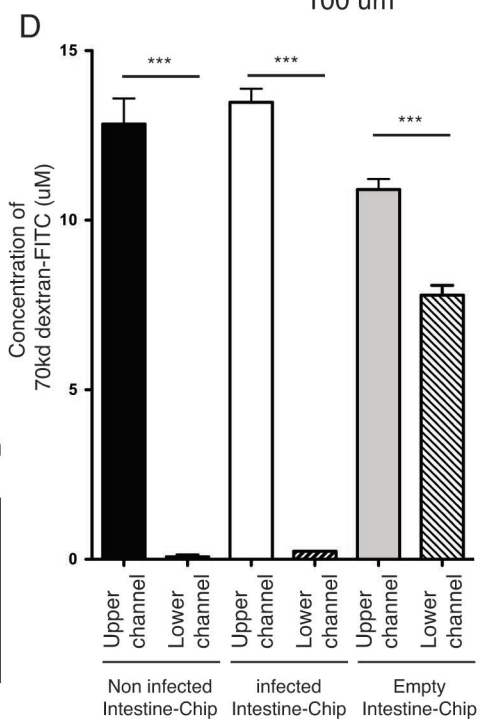
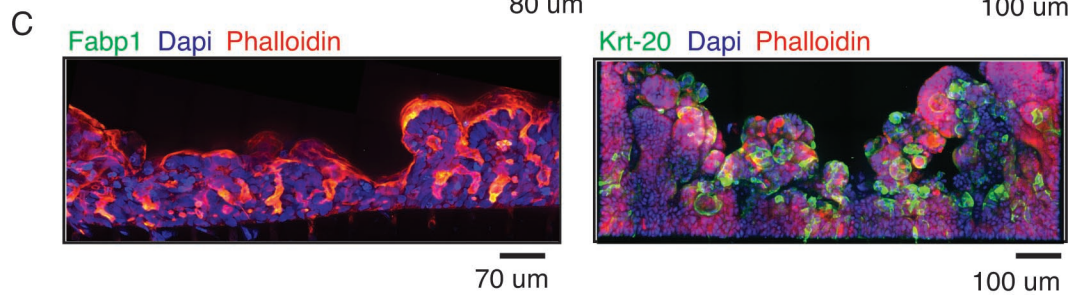
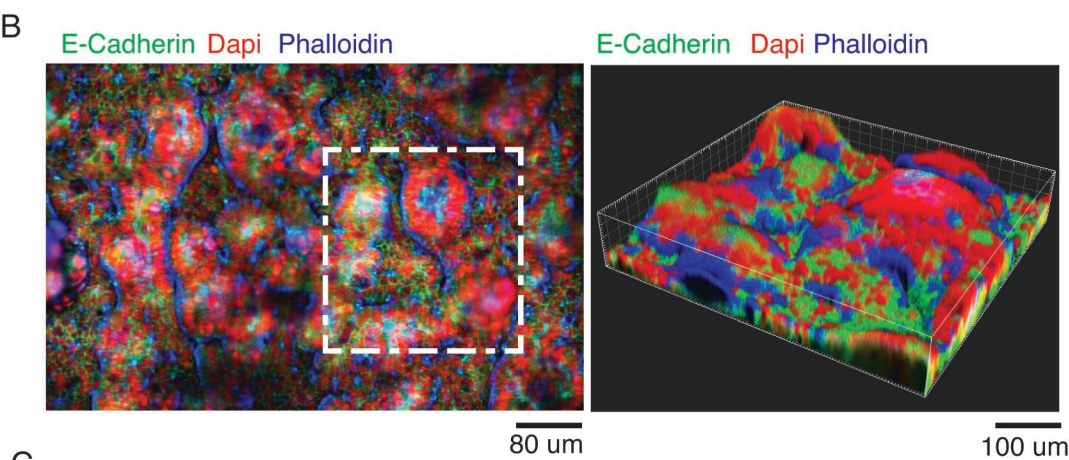
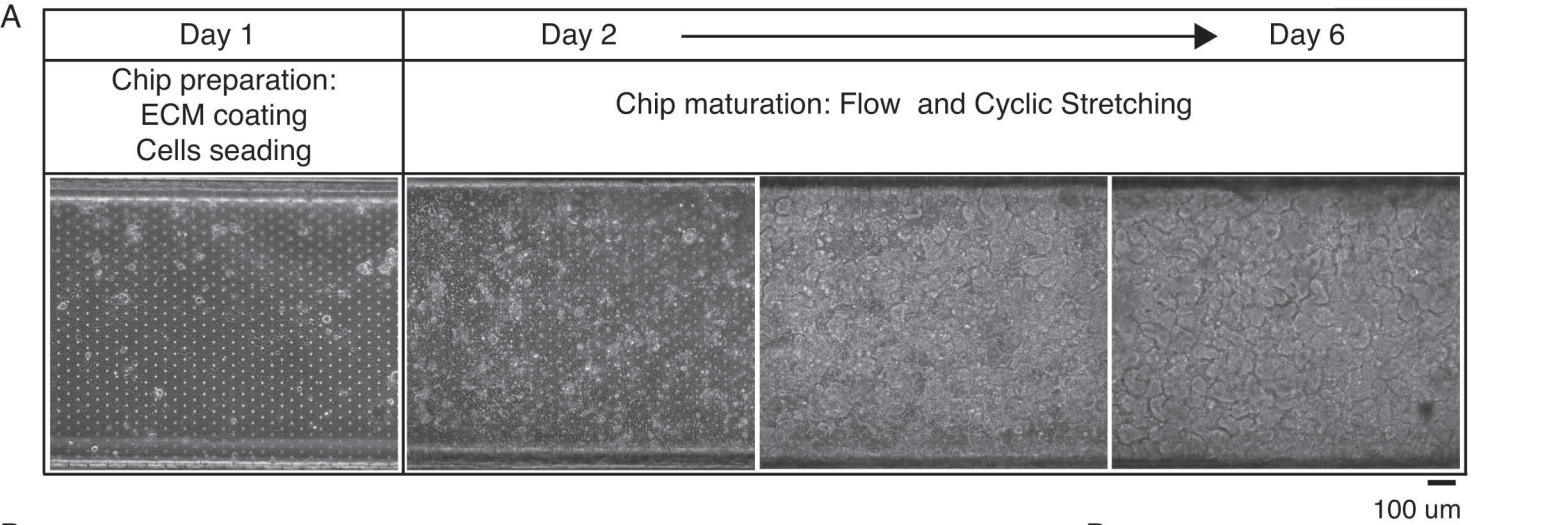
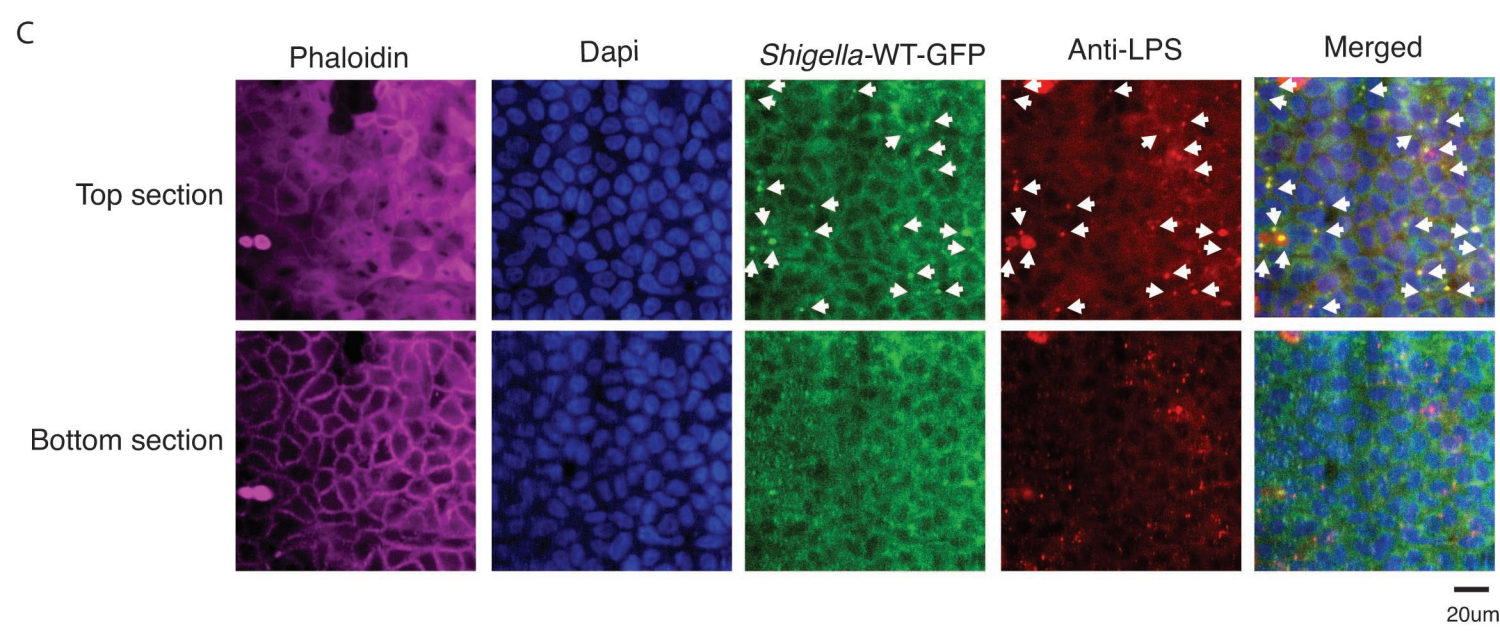
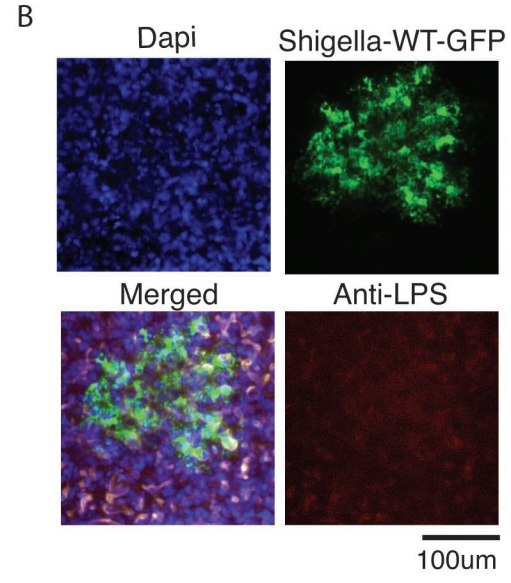
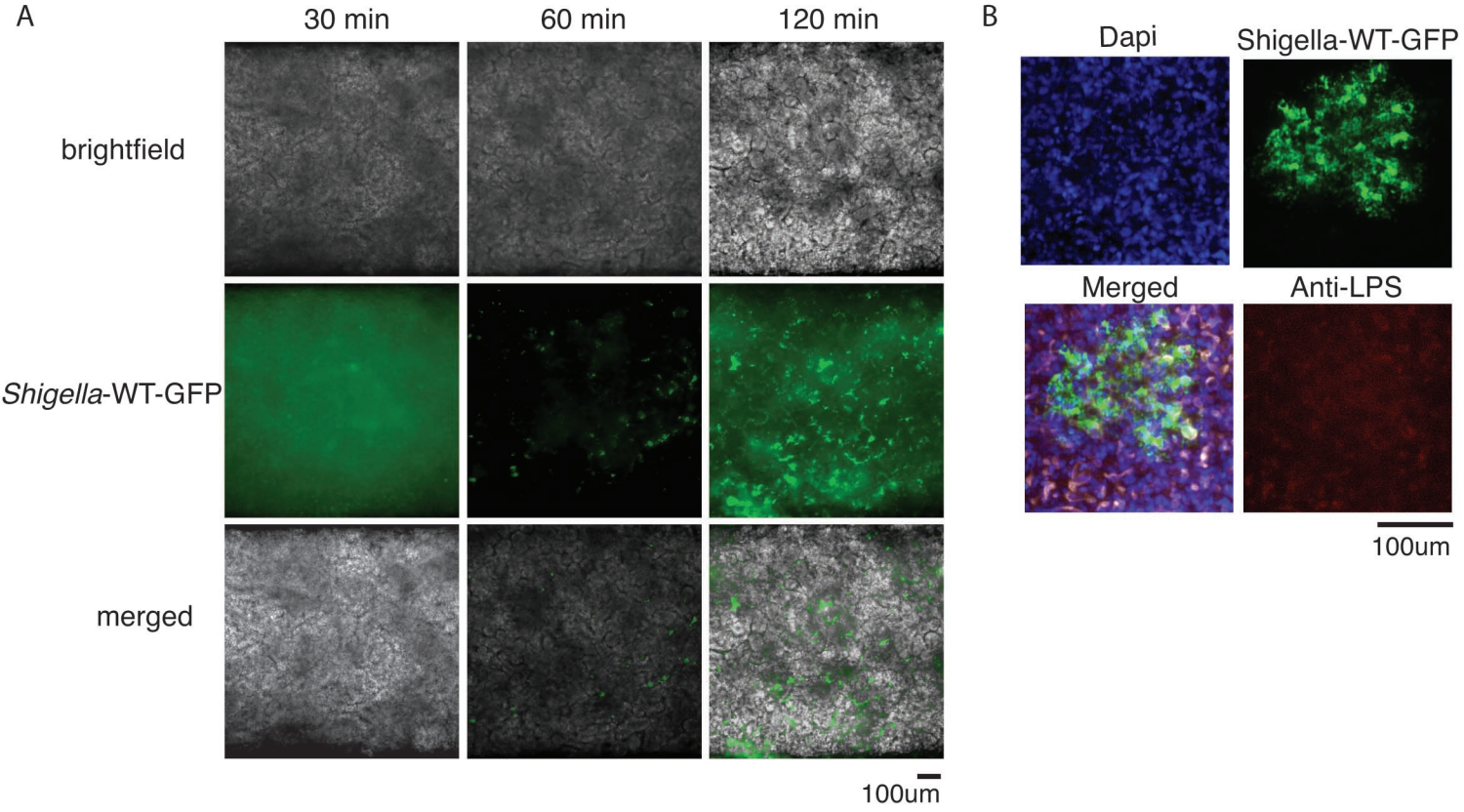


Figure 4



Supplementary Figure 1



Supplementary Figure 2

